QCD background for the UA1 $W \to t\bar{b}$ signal

A. Grosso and R. Odorico
Dipartimento di Fisica, Università di Bologna, I-40126 Bologna, Italy
and Istituto Nazionale di Fisica Nucleare, Sezione di Bologna, Bologna, Italy
(Received 19 December 1984)

The $c\bar{c}X$ and $b\bar{b}X$ background affecting the $W \to t\bar{b}$ $e/\mu + 2$ jets signal reported by the UA1 Collaboration is discussed. Calculations are based on an $O(\alpha_s^2)$ + leading-pole approximation scheme, which includes jet radiation in the initial and final states of the hard binary parton process, and include the heavy-flavor excitation contribution, the stability of which has been checked. The main conclusions are the following. (i) Selection cuts naturally induce a topological event structure on the surviving background mimicking that expected for a $W \to t\bar{b}$ signal. (ii) The background rates for $\mu + 2$ jets events, on which we concentrate, are compatible within theoretical uncertainties with the number of events experimentally observed. The importance of purely leptonic decay modes, which survive the lepton-isolation cuts, and the bias induced by lepton-isolation cuts on background event topologies are also clarified.

I. INTRODUCTION

The UA1 Collaboration has recently reported a signal for associated production of an isolated large-transverse-momentum lepton and two jets at the CERN $p\bar{p}$ collider.[1] The rate and features of the signal have been found to be inconsistent with expectations of charm- and bottom-quark decays, and to be in agreement with the process $W \to t\bar{b}$ followed by $t \to bl\nu$, where t is the sixth quark (top) of the weak Cabibbo current. The bounds $30 < m_t < 50$ GeV on the top-quark mass have also been reported.

The production of charm- and bottom-quark pairs can contaminate the above signal because of the possible presence of a third jet, due to QCD radiation, which allows the event to fake the $e/\mu + 2$ jets signal topology. Attention to this type of background was called originally in Ref. 2. Estimates of its contribution under selection cuts of a type similar to that eventually used[1] by UA1 have been made in Refs. 3 and 4. The background levels reported there are rather small (Ref. 3 quotes a $\sim 0.8\%$). However, UA1 uses cuts quantitatively different from those considered in Refs. 3 and 4, and the background appears to undergo order-of-magnitude variations by even relatively slight changes of the cut conditions. Also, in Refs. 3 and 4 only fusion production of $c\bar{c}X$ and $b\bar{b}X$ and just semileptonic decay modes of the heavy quarks have been considered.

The aim of this article is to present a determination of the $c\bar{c}X$ and $b\bar{b}X$ backgrounds surviving the specific cuts used by UA1 in isolating the "top" signal. In order to do that we perform a quantum-chromodynamics (QCD) calculation which includes parton radiation in the initial and final states. Besides considering the production of $c\bar{c}X$ and $b\bar{b}X$ via the fusion mechanism, we also include the heavy-flavor excitation contribution, for which we have verified the stability of the results in the kinematic regime of interest. In addition to semileptonic decay modes of c and b quarks, we also pay due attention to purely leptonic decay modes of these quarks, which escape e/μ isolation cuts rather easily.

II. THE QCD CALCULATION

A. General outline of the calculation

The calculations have been performed using the program COJETS, which simulates QCD in pp and $p\bar{p}$ production of jets and heavy flavors with the inclusion of initial and final QCD radiation. The program and its documentation have been published.[5] Its results for jet production have been compared with the relevant experimental data of the UA1 and UA2 collaborations.[6] Together with its companion program WIZJET, simulating pp and $p\bar{p}$ production of $W^{\pm}$ and Z^0 intermediate bosons in association with jets,[7] it has already been used to calculate leptonic signals of interest for $t\bar{t}$ and $W \to t\bar{b}$, $\bar{t}b$ and the corresponding $c\bar{c}X$ and $b\bar{b}X$ backgrounds.[2] We summarize here the main features of the calculation.

Besides computing the hard binary parton process in the $O(\alpha_s^2)$ approximation with the well-known matrix elements, initial and final radiations of QCD quanta are calculated in the leading-pole approximation (LPA) using the emission probability

$$dP_E = \frac{\alpha_s(K^2)}{2\pi} \frac{dK^2}{K^2} P(z)dz \ ,$$

where $P(z)$ is the splitting probability function appropriate to the given parton branching. The parton shower development is stopped when the virtual mass of the parton legs reaches a minimum value of $Q_0 = 3$ GeV. The parton mass cutoff regulates at the same time infrared and collinear divergences in the parton splitting probabilities, because of the ensuing kinematic bounds.[8,9] Initial QCD radiation, besides being responsible for the scale-development evolution of parton densities, represents an extra source of transverse momentum for the partons entering the hard process and generates jets off the initial state, which may have substantial transverse energies. For the QCD calculation of multiple-jet production the same approach has been used also in Ref. 10, with results quantitatively consistent with those[6,11] from COJETS as far as

the parton final state is concerned.

Quarks and gluons are fragmented independently according to the Field and Feynman model.[12] For heavy quarks the extension of the Field and Feynman model developed in Ref. 13 is used, adopting for the heavy-quark fragmentation function the form of Ref. 14. Decays of heavy-flavor particles are calculated according to Ref. 15, with finite-mass effects exactly taken into account.

The numerical results we present have been obtained with a value of 0.100 GeV for the QCD Λ parameter and a renormalizing K factor for parton densities equal to 2, following experimental indications[16] from UA1.

B. Heavy-flavor excitation

In order to perform the present calculations, COJETS has been extended to also include heavy-quark production by flavor excitation[17,18] ($gQ \to gQ$, $qQ \to qQ$). This represents a relatively simple adaptation of the program, which already treated QCD radiation off the initial state. It is the latter mechanism in fact which, via gluon evolution into heavy-quark pairs, drives the formation of the heavy-quark sea, off which flavor excitation takes place.

We have verified that the calculation of the flavor excitation contribution to $c\bar{c}X$ and $b\bar{b}X$ backgrounds is quite stable in the problem at hand. Well-known instabilities affect flavor excitation when calculating heavy-quark yields at small p_T. In fact, if the minimum-p_T cutoff $p_T^{\min}$ is small, the amount of heavy-quark sea evolved up to $p_T^{\min}$ considerably depends on the exact value of $p_T^{\min}$ and on the choice of the evolution scale. This uncertainty is then magnified in the cross-section calculation because of the divergent behavior of the flavor excitation matrix elements at small p_T. (In spite of that, for charm production it is possible to make the small-p_T calculation stable using experimental data on the p_T distribution of charmed hadrons, thus constraining the $p_T^{\min}$ cutoff, and on the charm structure function.[17]) In our case, though, the request of a large-p_T ($\gtrsim 12$ GeV/c) lepton resulting from the decay of the heavy quark automatically limits the calculation to only c and b quarks with large p_T. We are thus very far from the divergence at $p_T=0$ in the matrix elements, and, moreover, since the heavy-quark-sea evolution scale set by p_T is now large, the calculation of the heavy-quark-sea evolution only marginally depends on the exact choices for the initial and final values of the evolution scale. This is no longer true in a calculation involving top quarks yielding leptons of comparable p_T. If the top quark is very massive, in fact, the large p_T of the lepton can be predominantly contributed by the top-quark decay, and thus one should include in the calculation also top quarks produced at relatively small p_T. We shall not engage here in $t\bar{t}X$ calculations, however.

A proper calculation of the heavy-quark-sea evolution must of course include the kinematic constraint applying to the $g \to Q\bar{Q}$ branching:[17]

$$x_{\text{spect}} \geq x_{\text{act}} \frac{m_Q^2}{K^2} ,$$

where m_Q is the heavy-quark mass, K^2 the evolution variable, and x_{act} and x_{spect} are the momentum fractions carried by the spacelike heavy quark (which, after possible further evolution, will be active in the flavor excitation process) and the timelike heavy quark (which gives rise to a jet), respectively. With the QCD Monte Carlo approach, the constraint can be easily incorporated in the development of the initial evolution tree. Under the kinematic conditions implied by the UA1 cuts, though, the effect of such a finite-mass constraint on the level of the $c\bar{c}X$ and $b\bar{b}X$ flavor excitation background is not overwhelming. Eliminating it altogether would lead to an increase of the $b\bar{b}X$ background from this source by only a factor of ~ 2.5.

In our calculations for the $c\bar{c}X$ and $b\bar{b}X$ backgrounds to the UA1 top signal, the contribution from flavor excitation amounts to roughly ~ 1.5 that from fusion. This figure is rather independent of the value of the QCD parameter Λ. Therefore our results would not be qualitatively altered by neglecting flavor excitation altogether. Well understood, the importance of flavor excitation rises with the c.m. energy. For bottom, we find that its contribution at large p_T is about two times larger than that from fusion at 2 TeV, and the ratio between the two rises to ~ 5 at 20 TeV, and to ~ 10 at 40 TeV (the difference between pp and $p\bar{p}$ collisions is marginal). One should also keep in mind that the topological structures of the events from the two types of mechanisms have substantial differences.

A more complete discussion of the role of flavor excitation in the large-p_T production of heavy quarks will be presented elsewhere.[19]

C. Comparison with $O(\alpha_s^3)$ calculations

Comparable background calculations limited to the $2 \to 3$ processes gg (or $q\bar{q}$) $\to g Q\bar{Q}$ and $qg \to qQ\bar{Q}$ have been presented in Refs. 3 and 5 (in Ref. 4 heavy-quark masses in the QCD matrix elements have been neglected, however). It is, of course, of interest to compare the results from the $O(\alpha_s^3)$ approximation scheme with those from the one [$O(\alpha_s^2)$+LPA] considered here.

In Ref. 3 the $b\bar{b}X$ background under the $W \to t\bar{b}$ signal is estimated within the following cuts for lepton + 2 jets events: (1) $E_T(\text{lepton}) > 15$ GeV, (2) $E_T(\text{jet } 1) > 28$ GeV, (3) $E_T(\text{jet } 2) > 10$ GeV, (4) transverse hadronic energy within a cone having 30° of semiaperture around the lepton direction less than 5 GeV (lepton-"isolation" condition). A frozen coupling constant $\alpha_s = 0.15$ is used (with a "hard" scale of 81 GeV, it would correspond to $\Lambda = 0.35$ GeV), and the renormalizing K factor is apparently left to 1. The fragmentation function for heavy quarks of Ref. 14 is adopted. The bottom quark is left to decay semileptonically, $b \to c l \nu$, taking into account the finite mass of the c quark. The corresponding $p\bar{p} \to b\bar{b}X$ background to the above-defined lepton + 2 jets events is then found to have a cross section $\sigma = 10^{-4}$ nb at $\sqrt{s} = 540$ GeV (using presumably a semileptonic branching ratio of 0.1).[3] Under the same conditions our approximation scheme, limited to the fusion contribution alone, gives $\sigma = 0.9 \times 10^{-4}$ nb. The almost numerical coincidence should not be taken too seriously, of course.

We call attention to the fact that, in general, multiple radiation, which is missed in $O(\alpha_s^3)$ calculations, can

give rise to relevant effects. To illustrate that, let us mention that with the UA1 lepton + 2 jets selection cuts the mean transverse momentum of the (isolated) lepton + neutrino + 2 jets system is found to amount to ~ 6 GeV/c in our calculation (with a rather extended tail in the associated distribution). Such transverse momentum is generated by multiple radiation leading to jets falling below the experimental transverse-energy cut. This is no small number compared with the UA1 transverse-energy cuts on jets [E_T(jet) > 7, 8 GeV], and may give rise to important smearing effects and ensuing repopulation of otherwise statistically poor kinematic regions. In $O(\alpha_s{}^3)$ calculations, the above particle system comes out essentially balanced. Even if this particular source of transverse momentum is introduced by hand in the calculation, one is still left without the fluctuations in the internal topology of the lepton + 2 jets system expected from multiple radiation.

D. Leptonic and semileptonic decays of heavy-flavor particles

In the extensive literature covering possible leptonic signals for top particles attention has been exclusively devoted to semileptonic decay modes of the top particles, which one is looking for, and of the charm and bottom particles, which contribute the associated background.[2–4,20] Neglect of purely leptonic decays of heavy-flavor particles is apparently supported by the rather smallish theoretical estimates for their branching ratios. For instance, the $F \to \mu\nu$ branching ratio is estimated[21] to be about 100 times smaller than that for $F \to \mu X$. The branching ratio for $B_c \to \tau\nu_\tau$, where B_c is the pseudoscalar $b\bar{c}$ or $\bar{b}c$ state, is estimated[15] to be $\simeq 0.06$, which, compounded with a $B(\tau \to l\nu_l\nu_\tau) \simeq 0.18$, gives a $B(B_c \to l\nu_l\nu_\tau\nu_\tau) \simeq 0.01$. The relative contribution of this decay mode to the total lepton yield from bottom decays is further reduced by the fact that only a fraction of bottom quarks recombine with charm quarks to give B_c states.

What is neglected in these considerations, however, is that (i) "trigger-bias" effects associated with requiring the leptons to have a large p_T can alter the relative importance of the contributions from the various decays, and (ii) the "isolation" cut on the lepton, aimed to enhance the top signal, while on one hand suppresses the contribution from semileptonic decays of charm and bottom particles, on the other hand, leaves the purely leptonic decays to contribute a comparatively larger share of the surviving background. In order to illustrate the relevance of point (i), we plot in Fig. 1 the ratio of $d\sigma(F \to \mu\nu)/dp_T(\mu)$ to $d\sigma(D \to \mu X)/dp_T(\mu)$ at large $p_T(\mu)$, assuming $\sigma(D) = 2\sigma(F)$ and $B(F \to \mu\nu) = 10^{-2} B(D \to \mu X)$. The ratio of $\frac{1}{200}$ between the total cross sections times branching ratios is reduced to a mere $\sim \frac{1}{10}$ for $p_T(\mu) \gtrsim 10$ GeV/c. Muon isolation requirements will increase this ratio further.

When considering the $c\bar{c}X$ and $b\bar{b}X$ backgrounds to the top leptonic signal, therefore, due consideration must be given to purely leptonic decay modes. As a result, the background acquires a rather composite structure, which may lead to the fictitious manifestation of new "sources" when imposing strict event selection criteria.

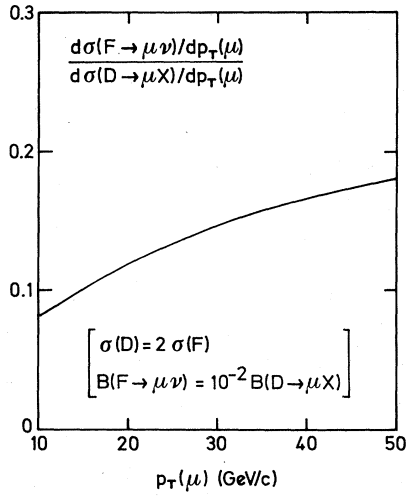

FIG. 1. Ratio of inclusive μ yields from production and leptonic decay of F mesons and production and semileptonic decay of D mesons as a function of the transverse momentum $p_T(\mu)$. A total cross-section ratio $\sigma(D)/\sigma(F) = 2$ and a ratio between branching fractions $B(F \to \mu\nu)/B(D \to \mu X) = 10^{-2}$ are assumed.

E. UA1 event-selection cuts

Two different sets of cuts have been used[1] by UA1 to select electron + 2 jets and muon + 2 jets candidates for $W \to t\bar{b}$, $t \to lX$.

For electron + 2 jets events, the selection demands the following: (1) an electron with $E_T > 15$ GeV and pseudorapidity $|\eta| < 1.5$; (2) a transverse-energy deposition and a $\sum p_T$ for charged tracks within a cone

$$\Delta R = (\Delta\eta^2 + \Delta\phi^2)^{1/2} < 0.4$$

around the electron direction both less than 1 GeV (η being the pseudorapidity and ϕ the azimuth measured in radians); (3) an angle $\theta^*_{j_2}$ of the lowest-E_T jet with the average beam axis in the electron + 2 jets rest frame having $|\cos\theta^*_{j_2}| < 0.8$; and (4) a transverse-energy component of the electron perpendicular to the plane formed by the $p\bar{p}$ axis and the highest-E_T jet, E_T^{out}, larger than 8 GeV.

For μ + 2 jets events the following has been required: (1) a muon with $p_T(\mu) > 12$ GeV/c and pseudorapidity $|\eta| < 1.5$; (2) a transverse-energy deposition $\sum E_T < 0.2\, p_T(\mu)$ and a sum over charged-particle momenta $\sum p_T < 0.1\, p_T(\mu)$, where the sums are extended to a cone with $\Delta R < 0.4$ around the muon direction; and (3) no jet within $\Delta R = 1$ from the muon.

Jets are requested to lie within $-2.5 < \eta < 2.5$, and to have a transverse energy $E_T > 8$ GeV for the higher-E_T jet (j_1), and $E_T > 7$ GeV for the lower-E_T jet (j_2). The angular resolution ΔR for jets is set at $\Delta R = 1$.

The above selection cuts are all easily implementable in our calculation. Because of the poor angular resolution used by UA1 in defining the jets, we have not found it necessary to carry out the fragmentation of the QCD quanta, except of course for the heavy quark generating the lepton. Quanta which are distant by less than $\Delta R = 1$ have been grouped together so as to form a unique jet.

Effects from the grouping, though, are marginal, and essentially the same results are obtained considering each quantum as a single jet.

III. BACKGROUND SHAPE

In Ref. 1 the $W \to t\bar{b}$, $t \to lX$ hypothesis for the lepton + 2 jets signal has been advocated largely on the basis of the observed kinematic distributions and, in particular, of the observed aggregation of the three electron + 2 jets events and of the three muon + 2 jets events around invariant-mass values for the $(l\nu_T j_1 j_2)$ and $(l\nu_T j_2)$ systems of about 80 and 40 GeV, respectively.

The UA1 selection cuts obviously cause the invariant masses $M(l\nu_T j_1 j_2)$ and $M(l\nu_T j_2)$ to have some minimum values, independently of the source of the events. On the other hand, conventional large-p_T dynamics suppresses large values for them. Therefore it is to be expected, on general grounds, that the $c\bar{c}X$ and $b\bar{b}X$ backgrounds surviving the cuts will be concentrated in some limited intervals of $M(l\nu_T j_1 j_2)$ and $M(l\nu_T j_2)$. It remains to see how wide the intervals are, and around which values they are centered.

In order to clarify this point we have considered a background source with an essentially model-independent decay dynamics and which certainly survives the lepton isolation cuts: $p\bar{p} \to b\bar{b}X$ with a b quark fragmenting into B_c, and a subsequent decay $B_c \to \tau\nu_\tau$, $\tau \to l\nu\nu_\tau$, B_c being the pseudoscalar $(b\bar{c})$ or $(\bar{b}c)$ state. We plot in Fig. 2 the distributions for this background in the invariant masses $M(lj_1 j_2)$, $M(lj_1)$, and $M(lj_2)$ after imposition of the UA electron cuts, as specified in Sec. II E. Figure 3 shows the corresponding distributions in $M(l\nu_T j_1 j_2)$ and $M(l\nu_T j_2)$.

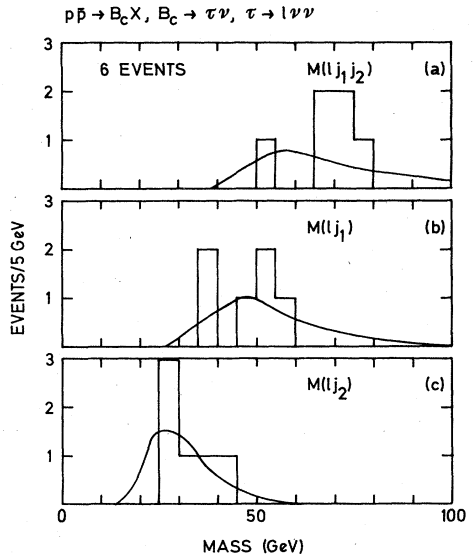

FIG. 2. Invariant-mass distributions for lepton-jets combinations in $p\bar{p} \to b\bar{b}X$, $B_c \to \tau\nu$, $\tau \to l\nu\nu$ events surviving the UA1 electron cuts. Experimental data refer to the six e/μ+2 jets UA1 events. (a) Distribution in the invariant mass of the lepton + 2 jets system. (b) Distribution in the invariant mass of the lepton + highest-E_T jet system. (c) Distribution in the invariant mass of the lepton + lowest-E_T jet system.

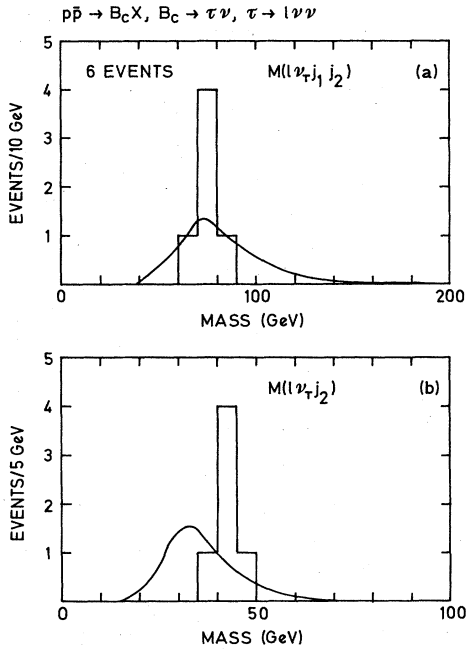

FIG. 3. Same as in Fig. 2 for (a) invariant mass of the lepton + 2 jets + missing transverse energy (ν_T) system, (b) invariant mass of the lepton + ν_T + lowest-E_T jet system.

From the comparison with the UA1 data it appears that the clustering of the events around the observed values may have a rather conventional explanation.

The shapes of the background distributions considerably depend on the positions of the cuts. Softening the cuts, the distributions shift to lower-mass values, whereas more stringent cuts move them to higher-mass values. With higher statistics, allowing for more penalizing selection criteria, one should therefore be able to discriminate between the background and a genuine signal, at least in principle.

IV. BACKGROUND RATES

Electron identification in the UA1 experiment involves a complex procedure (matching within a certain tolerance of the calorimetric measurement with the track measurement, study of the shape of the electromagnetic shower, etc.). In the presence of appreciable jet activity and without the requirement of a large missing transverse energy (as in the case of $W \to l\nu$ events) discussion of the background becomes more delicate. In particular, to make serious estimates of the $c\bar{c}X$ and $b\bar{b}X$ backgrounds which may survive because of the gap between the minimum transverse energy deposition $E_T = 15$ GeV and the minimum track momentum $p_T = 7$ GeV/c required for the electron candidate would need a thorough simulation of the experimental apparatus. One can think, for instance, of the contamination from $F \to e\nu\eta$, $\eta \to \gamma\gamma$, with the two γ almost collinear to the electron, so as to fake an electron shower with $E_T > 15$ GeV, whereas the true electron is requested to have only a $p_T > 7$ GeV. The effective lowering of the p_T cutoff on the electron would cause a considerable increase of this background contribution in

the calculation. The actual result would strongly depend on how much the two γ should be collimated with the electron so as to be seen by the detector as a single-electron shower. Similar considerations may apply to other semileptonic decay modes of charm and bottom particles. Even if the relevant decay modes may be rare in absolute, their presence can appreciably reduce the effectiveness of the otherwise strong suppressions induced by the isolation cuts.

Therefore we limit the discussion of background rates to the calculationally more tractable case of $\mu+2$ jets events.

The most uncertain part in the calculation of background rates is represented by the fragmentation functions of heavy quarks. Adopting for the fragmentation function $D_Q(z)$ the functional form of Ref. 14,

$$D_Q(z) \propto \left[z \left[1 - \frac{1}{z} - \frac{\epsilon_Q}{1-z} \right]^2 \right]^{-1},$$

the $D_Q(z)$ shape is parametrized by ϵ_Q. The smaller ϵ_Q is, the harder the $D_Q(z)$ shape. According to the experimental survey of Ref. 22, $0.1 \lesssim \epsilon_c \lesssim 0.75$ for charmed quarks, and $0.001 \lesssim \epsilon_b \lesssim 0.08$ for bottom quarks. Because of the importance of the $b\bar{b}X$ background, the uncertainty in ϵ_b generates an imprecision by a factor ~ 3 in the predicted rates. We have fixed ϵ_b by using the μ inclusive cross section $d\sigma/dp_T(\mu)$ as measured by UA1 (Ref. 1). In order to fit the data, which are quoted to have a $\lesssim 25\%$ contamination from pion and kaon decays, a rather low value for ϵ_b is needed. The fit in Fig. 4 corresponds to $\epsilon_b = 0.001$. We have kept this value for calculating the $b\bar{b}X$ background rates to $\mu+2$ jets events. For the charm contribution we have used $\epsilon_c = 0.25$.

As already discussed in Sec. II D, the heavy-quark background has a composite nature. Since the lepton-isolation requirement suppresses the contribution of semileptonic decay modes, purely leptonic decay modes, whose importance is already increased by the large-p_T selection for the lepton, may turn out to contribute a substantial share of the surviving background. We shall not engage here in an exhaustive discussion of all possible $c\bar{c}X$ and $b\bar{b}X$ background sources. Rather, we will concentrate on a few which are likely to have a role in the background buildup, and which conveniently illustrate the variety of potential sources. All the results we quote apply to the UA1 muon cuts, as specified in Sec. II E. The $\mu+2$ jets event rates we quote refer to an integrated luminosity of 120 nb^{-1}, corresponding to that of the UA1 sample.[1]

We first consider purely leptonic decay modes, which easily escape the μ isolation requirements. Also, results for them are less dependent on the particle conversion model for the heavy quarks.

For $F^{\pm}$ charmed particles the $F \to \mu\nu$ decay mode is expected to have a branching ratio $B = 10^{-3}$, approximately (see, e.g., Ref. 21), which is the value we assume in the calculation. Using the experimental indications that at large p_T particle yields tend to be relatively independent of quantum numbers, we assume that $\frac{1}{3}$ of large-p_T charm quarks convert into $F^{\pm}$. The corresponding background contribution to the UA1 $\mu+2$ jets sample that we obtain is of about 0.15 events, to be compared with the experimentally observed 3. The non-negligible contribution from this charm decay mode is due to the relative enrichment caused by the high-p_T lepton selection. In itself, this contribution does not appear to be very dangerous, but gives an idea of how selection cuts can bring into play even very rare decay modes.

Also bottom particles can undergo purely leptonic decays. We consider as an example the $(b\bar{c})$ and $(\bar{b}c)$ pseudoscalar states $B_c^{\pm}$, which can decay $B_c \to \tau\nu_\tau$, with an expected[15] $B \simeq 0.06$. The τ can subsequently decay $\tau \to \mu\nu_\mu\nu_\tau$, with a measured[23] $B = 0.185$. One can thus have events with the μ accompanied only by neutrinos in the bottom decay. Assuming, as for $F^{\pm}$, that at large p_T particle yields tend to be independent of quantum numbers, we assume that $\frac{1}{4}$ of large-p_T bottom quarks convert into a B_c state. The background rate that we obtain from this channel, then, is of about 0.4 events.

Let us now turn to semileptonic decays of bottom quarks. In this case one is much more dependent on the b-quark fragmentation and decay model when estimating the fraction of $b\bar{b}X$ events which survive the μ-isolation cuts. With the extended Field-Feynman model specified in Sec. II A and a semileptonic branching ratio $B = 0.1$, we find that the rate for events of this type, which survive the UA1 muon cuts, is appreciable and amounts to about two events, to be compared with the experimentally observed three.

For all the three decay channels considered the contribution from heavy-flavor excitation is about 1.5 times that of fusion. Therefore, although flavor excitation appreciably increases the event rates, the results do not qualitatively depend on it.

In concluding this section, we would like to stress that those presented are theoretical estimates which are affected by the ambiguities of the particle-conversion model used and by the intrinsic uncertainties of the QCD calculation.

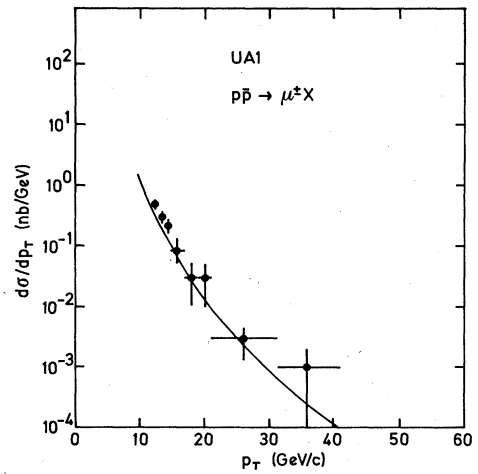

FIG. 4. Fit to the muon inclusive $d\sigma/dp_T(\mu)$ differential cross section as measured by UA1 (Ref. 1). (The contamination from K and π decays is quoted to be $\lesssim 25\%$.)

V. BIAS IN THE EVENT TOPOLOGIES INDUCED BY THE MUON-ISOLATION CUT

One might hope to establish evidence for a new source of $\mu+2$ jets events by exploiting an observed change in the kinematic distributions induced by the μ isolation cut on the experimental event sample, and bypass in this way the unfavorable theoretical estimates (and associated uncertainties) for the $c\bar{c}X$ and $b\bar{b}X$ background.[1] One should not be simplistic about that, though, and believe that, except for the detailed fragmentation features of the heavy quark into the muon and other debris, the mean $c\bar{c}X$ and $b\bar{b}X$ event topologies are the same before and after the μ isolation cut.

Let us consider $b\bar{b}X$ events, with the bottom quark decaying semileptonically. Figure 5 shows the distributions in $\hat{p}_T$, the parton transverse momentum generated in the hard binary parton process, when the UA1 muon cuts are imposed with and without the μ isolation requirement. After μ isolation is required there is a marked softening of the distribution, with consequent changes in the event topologies. The $\hat{p}_T$ softening is easy to understand. In order to pass the isolation cut the b jet debris must carry a total transverse energy small with respect to $p_T(\mu)$. Thereby, one favors topologies in which the μ takes an energy fraction larger than usual in the fragmentation-decay process, and as a consequence at a given $p_T(\mu)$ one favors topologies in which the primary b quark has a transverse momentum smaller than usual. The shift of $\hat{p}_T$ to lower values directly entails modifications in the characteristics of QCD radiation, since $\hat{p}_T$ represents the "hard scale" controlling QCD emission. In order to get an extra radiation jet surviving the cuts, the radiation process is now forced toward less probable kinematic configurations.

One would feel less uneasy about such changes if the relevant kinematic distributions were stable toward the relative proportions of initial and final radiations in contributing the second jet. The azimuthal distance $\Delta\phi(\mu j_1)$ between the muon and the highest-E_T jet has distributions practically identical for the two classes of events, in which the lowest-E_T jet j_2 is originated by initial and by final radiations. But for $\cos\theta^*_{j_2}$, where $\theta^*_{j_2}$ is the angle between the average beam axis and j_2 in the $(\mu j_1 j_2)$ rest frame, differences are larger [Fig. 6(b)]. For initially radiated j_2 there is a peak near $|\cos\theta^*_{j_2}|\simeq 1$, whereas for finally radiated j_2 the distribution is much more uniform and not far from that expected for $W\to t\bar{b}$, $t\to\mu X$. With limited statistics the $\Delta\phi(\mu j_1)$ distribution is not of great help in discriminating a $W\to t\bar{b}$ signal from background, as is clear from Fig. 6(a). Much more helpful in this sense would be the $\cos\theta^*_{j_2}$ distribution, if the $b\bar{b}X$ background were limited to the initial-radiation contribution. But this does not appear to be the case. The contributions from initial and final radiations turn out to be comparable. The final theoretical result for $dN/d\cos\theta^*_{j_2}$ crucially depends on the exact relative proportions of these two components.

When attempting to calculate the changes in the relative proportions of initial and final radiations, and thus in $dN/d\cos\theta^*_{j_2}$, induced by the imposition of the μ isolation cut, one becomes highly sensitive to the intrinsic ambiguities of the QCD calculation, and in particular to the choice of the scales entering the running coupling constant and controlling the phase space available for emission. It should be clear that such ambiguities do not affect only the $O(\alpha_s{}^2)$+LPA approximation scheme used

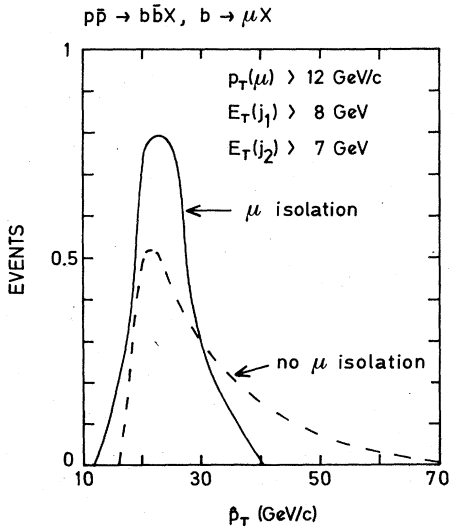

FIG. 5. Distribution in the parton-transverse momentum $\hat{p}_T$ generated in the hard binary parton process for Monte Carlo events $p\bar{p}\to b\bar{b}X$, $b\to\mu X$ which survive the UA1 muon cuts, with and without the μ isolation cut.

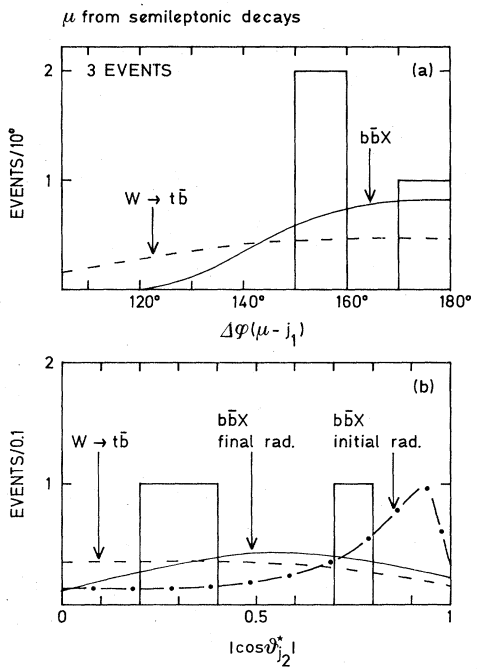

FIG. 6. Distributions for $p\bar{p}\to b\bar{b}X$, $b\to\mu X$ events surviving the UA1 muon cuts compared to corresponding results for $p\bar{p}\to WX$, $W\to t\bar{b}$, $t\to\mu X$ ($m_{\rm top}=40$ GeV) and to the UA1 $\mu+2$ jets data. (a) Distribution in the azimuthal distance between the lepton and the highest-E_T jet. (b) Distribution in $|\cos\theta^*_{j_2}|$, where $\theta^*_{j_2}$ is the angle between the lowest-E_T jet and the mean beam axis in the $\mu+2$ jets rest frame.

here, but are present also in an $O(\alpha_s^3)$ scheme, although there they can be disguised. In the latter scheme α_s cannot be left to run with the varying vertex kinematics, because otherwise gauge invariance could not be preserved. But of course higher-order terms will cause α_s to run with the vertex kinematics, as in the $O(\alpha_s^2)+$LPA scheme, and their impact can turn out to be quite different in the spacelike and in the timelike regimes, as it has been well illustrated by K factor calculations.

In conclusion, the effects of the μ-isolation cut on some kinematic distributions which crucially depend on details of the QCD dynamics, like $dN/d\cos\theta^*_{j_2}$, cannot be reliably calculated with the current QCD approximation schemes.

VI. CONCLUSIONS

We have called attention to a number of points concerning the $c\bar{c}X$ and $b\bar{b}X$ background to the $e/\mu+2$ jets signal reported by the UA1 Collaboration.

(i) The cuts used[1] by UA1 appear to induce a concentration of the surviving background events around values for the invariant masses of the $(l\nu_\tau j_1 j_2)$ and $(l\nu_\tau j_2)$ systems not very far from those expected for a $W \to t\bar{b}$ signal. Evidence for such a signal, therefore, cannot exclusively rest on experimental observation of kinematic correlations of this type.

(ii) Background rates for $\mu+2$ jets events (on which we have concentrated because of difficulties in handling a proper background calculation of $e+2$ jets events) appear to be compatible, within the uncertainties of the calculation, with the experimental event rates (see Table I). One should pay attention to the fact that even relatively small changes of the selection cuts considerably affect the background level.

(iii) Purely leptonic decay modes of c and b quarks, in spite of their modest branching ratios, can contribute a substantial fraction of the background (Table I). This is in part a side effect of the large-p_T selection for the lepton, and also a direct consequence of the fact that such decays easily escape the lepton-isolation cut.

(iv) When comparing event topologies before and after the μ-isolation cut, one should be aware that such a cut not only entails a selection on the fragmentation-decay mode, but also induces considerable alterations in the topological structure of background events. Because of the comparable importance of initial and final QCD radiations in generating the second (lowest-E_T) jet, and the rather different shapes of the contributions from these two components to some key distributions, one should be cautious in coming to conclusions when observing changes in such distributions induced by the lepton-isolation cut. The change may be simply due to a modification of the relative proportions of initial and final radiations caused by the cut.

It appears from what we have seen that the analysis of correlations is of paramount importance in isolating a top signal from the underlying background. The exhaustive exploitation of correlations inside the events when comparing with simulated background can significantly improve the chances of establishing evidence for "new sources." When dealing with events having relatively complex topologies, as in our case, the delicate choice of effective event selection criteria can be considerably helped by well-known statistical techniques of pattern analysis.[24] For example, the complications outlined in the above point (iv) could have been at least in part overcome in this way.

TABLE I. $p\bar{p} \to c\bar{c}X$, $b\bar{b}X$ background event rates applying to the UA1 muon cuts (Sec. II E) and to an integrated luminosity of 120 nb^{-1}, for various charm and bottom decay channels. The background event rates are to be compared with the three $\mu+2$ jets events observed by UA1.

Decay channel	Events
$F \to \mu\nu$	0.15
$B_c \to \tau\nu$, $\tau \to \mu\nu\nu$	0.40
$b \to \mu X$	2.00

Note added

The paper contains a quantitative comparison with the calculation of Ref. 3. We have refrained from presenting a similar comparison with the calculation of Ref. 4, since in the latter the dependence of matrix elements on the finite masses of heavy quarks is not taken into account. A simple order-of-magnitude comparison, however, is possible. The cuts assumed in Ref. 4 are not very different from those eventually adopted by UA1 for μjj events: $p_T(\mu) > 8$ GeV, $E_T > 8$ GeV for both jets, and a muon isolation condition. With such cuts the $b\bar{b}X$ background to isolated $\mu+2$ jets events at $\sqrt{s} = 540$ GeV is estimated to have a cross section of $\sigma = 16$ pb [Eq. (4) in Ref. 4], which coupled with the UA1 integrated luminosity of 0.12 pb^{-1}

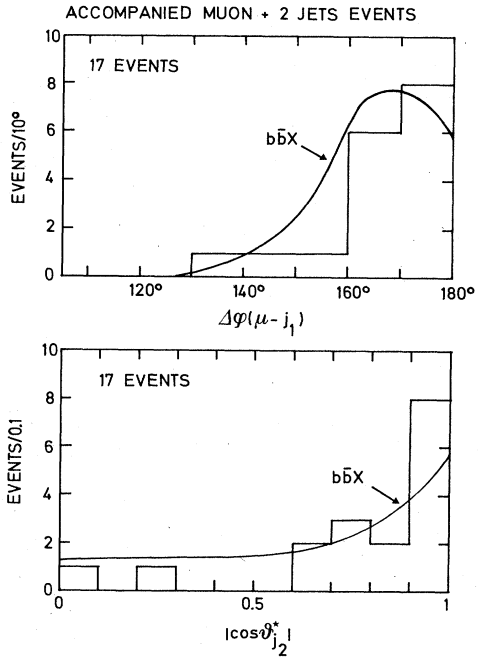

FIG. 7. Comparison of theoretical results with kinematic distributions for the sample of UA1 μjj events with accompanied muon (comparison in shape and normalization). Kinematic variables are the same as in Fig 6.

gives a rate of 1.92 events. This is to be compared with the 0.8 event we obtain with the UA1 muon cuts from the fusion process and semileptonic decays alone. In order to make the comparison quantitative one should correct for a series of effects (i) the difference of the cuts from those of UA1, (ii) the dependence of the matrix elements on the finite masses of heavy quarks, and (iii) the different fragmentation function for bottom quarks, which we have found is not hard enough to reproduce the muon inclusive $d\sigma/dp_T$ cross section measured by UA1. In addition, one should not forget that in Ref. 4 multiple QCD radiation effects are neglected. Contrary to Ref. 3, where cuts at much larger E_T are considered, it is likely that such effects are important in the kinematic regime discussed in Ref. 4.

Weaknesses in the "empirical" estimate of the $b\bar{b}X$ background made in Ref. 1 are discussed at length in Sec. V of the paper. Since such an estimate is based on the kinematic characteristics of accompanied $\mu+2$ jets events, we have added Fig. 7 in order to show the comparison (in shape and normalization) of the results from our calculation with the experimental distributions for such a sample of events. Final QCD radiation is calculated assigning a virtual mass squared of $\frac{3}{4}Q^2$ to the final parton legs, where $Q^2=2\hat{s}\hat{t}\hat{u}/(\hat{s}^2+\hat{t}^2+\hat{u}^2)$ is the Field-Feynman-Fox variable ($\simeq\hat{p}_T{}^2$ at c.m. $\cos\hat{\theta}$ sufficiently away from 0). Such a prescription yields a ratio of (accompanied) μjj events originating from final radiation to those originating from an initial radiation of $\simeq 0.25$. The prescription makes sure that virtual masses independently generated for the two parton legs in the QCD cascades are always consistent with the kinematic limit. It does not saturate the latter, however. Assigning instead a virtual mass squared of $3Q^2$, thus saturating the kinematic limit and taking care at the same time of rejecting generated pairs of virtual masses inconsistent with it, the above ratio rises to $\simeq 0.65$. As pointed out in the paper, while the $\Delta\phi(\mu-j_1)$ distribution little depends on this ratio, the shapes of the two contributions to the $\cos\theta^*_{j_2}$ distribution are quite different. Because of the theoretical uncertainties in determining this ratio and since its value can change under the bias on the production mechanism induced by the isolation cut (see Fig. 5 and the associated discussion), it does not appear possible to have a safe theoretical anticipation of the $\cos\theta^*_{j_2}$ distribution for isolated $\mu+2$ jets events, even constraining the calculation to fit the same distribution for nonisolated $\mu+2$ jets events.

In Ref. 1 a comparison between the distributions in the invariant mass $M(\mu\nu_T j_1 j_2)$ of the "isolated" and the "accompanied" μjj events is used to establish model-independent evidence for the signal. Besides the 3 isolated μjj events only 5 accompanied μjj events [of the 17 shown, e.g., in Fig. 6(a) of Ref. 1] are considered in the comparison made in Fig. 7(a) of Ref. 1. If one leaves apart just one entry in Fig. 7(a), the one with highest mass, all other (7) entries are comprised within ± 12 GeV from a center at ~ 68 GeV. That should be compared with the systematic error of ± 10 GeV in the mass evaluation quoted at the end of Sec. V in Ref. 1. Therefore, the closer clustering in mass of the 3 isolated events, within ± 3 GeV, cannot be considered significant.

The assumption that at large p_T (>20 GeV) yields of bottom particles are approximately independent of other quantum numbers implies the existence of a nonperturbative source of charm quarks. It should be clear that the assumption only demands that such a source is active when the phase space available for fragmentation is large with respect to the charm-quark mass, so that phase-space constraints act approximately in the same way for u,d,s, and c quarks.

[1] G. Arnison *et al.* (UA1) Collaboration), Phys. Lett. **147B**, 493 (1984).

[2] G. Ballocchi and R. Odorico, Phys. Lett. **136B**, 126 (1984); R. Odorico, Nucl. Phys. **B242**, 297 (1984).

[3] I. Schmitt, L. M. Sehgal, H. Tholl, and R. M. Zerwas, Phys. Lett. **139B**, 99 (1984).

[4] V. Barger, H. Baer, K. Hagiwara, A. D. Martin, and R. J. N. Phillips, Phys. Rev. D **29**, 1923 (1984).

[5] R. Odorico, Comp. Phys. Commun. **32**, 139 (1984); **34**, 431(E) (1985).

[6] R. Odorico, Nucl. Phys. **B228**, 381 (1983); **B244**, 313 (1984).

[7] R. Odorico, Comp. Phys. Commun. **32**, 173 (1984); **34**, 437(E) (1985).

[8] R. Odorico, Nucl. Phys. **B172**, 157 (1980).

[9] G. C. Fox and S. Wolfram, Nucl. Phys. **B168**, 285 (1980).

[10] R. D. Field, G. C. Fox, and R. L. Kelly, Phys. Lett. **119B**, 439 (1982).

[11] R. Odorico, Phys. Lett. **118B**, 151 (1982).

[12] R. D. Field and R. P. Feynman, Nucl. Phys. **B136**, 1 (1978).

[13] T. Sjöstrand, University of Lund Report NO. LU TP 79-8, 1979 (unpublished).

[14] C. Peterson, D. Schlatter, I. Schmitt, and P. M. Zerwas, Phys. Rev. D **27**, 105 (1983).

[15] A. Ali, J. G. Körner, G. Kramer, and J. Willrodt, Z. Phys. C **1**, 203 (1979); Nucl. Phys. **B168**, 409 (1980). A. Ali and E. Pietarinen, *ibid.* **B154**, 519 (1979).

[16] G. Arnison *et al.* (UA1 Collaboration), Phys. Lett. **136B**, 294 (1984).

[17] R. Odorico, Phys. Lett. **107B**, 271 (1981); Nucl. Phys. **B209**, 77 (1982); Phys. Lett. **118B**, 425 (1982).

[18] B. L. Combridge, Nucl. Phys. **B151**, 429 (1979). V. Barger, F. Halzen, and W. Y. Keung, Phys. Rev. D **25**, 112 (1982).

[19] A. Grosso and R. Odorico (in preparation).

[20] V. Barger, A. D. Martin, and R. J. N. Phillips, Phys. Lett. **125B**, 339 (1983); **125B**, 343 (1983); Phys. Rev. D **28**, 145 (1983); V. Barger *et al.*, *ibid.* **29**, 887 (1984); V. Barger and R. J. N. Phillips, *ibid.* **30**, 1890 (1984). R. M. Godbole, S. Pakvasa, and D. P. Roy, Phys. Rev. Lett. **50**, 1539 (1983); F. Halzen and D. M. Scott, Phys. Lett. **129B**, 341 (1983); L. M. Sehgal and P. M. Zerwas, Nucl. Phys. **B234**, 61 (1984); K. Hagiwara and W. F. Long, Phys. Lett. **132B**, 202 (1983); R. Horgan and M. Jacob, Nucl. Phys. **B238**, 221 (1984); D. P. Roy, Z. Phys. C **21**, 333 (1984); V. A. Khoze and M. A. Shifman, Usp. Fiz. Nauk. **140**, 3 (1983) [Sov. Phys. Usp. **26**, 387 (1983)].

[21] M. K. Gaillard, B. W. Lee, and J. Rosner, Rev. Mod. Phys.

47, 277 (1975).

[22]J. Dorfan, in *Proceedings of the 1983 International Symposium on Lepton and Photon Interactions at High Energies, Ithaca, New York,* edited by D. G. Cassel and D. L. Kreinick (Newman Laboratory of Nuclear Studies, Cornell University, Ithaca, 1983), p. 686.

[23]Particle Data Group (M. Aguilar-Benitez *et al.*), Rev. Mod. Phys. **56**, S1 (1984).

[24]R. Odorico, Phys. Lett. **120B**, 219 (1983); G. Ballocchi and R. Odorico, Nucl. Phys. **B229**, 1 (1983).